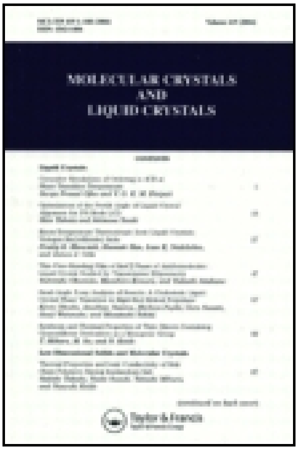

Molecular Crystals and Liquid Crystals

Publication details, including instructions for authors and subscription information:
http://www.tandfonline.com/loi/gmcl16

The Search for Quantum Liquid Crystals

Sujane C. Wang [a], Legesse Senbetu [a] & Chia-Wel Woo [a]

[a] Department of Physics, University of California, San Diego La Jolla, California, 92093, U.S.A.

To cite this article: Sujane C. Wang, Legesse Senbetu & Chia-Wel Woo (1981): The Search for Quantum Liquid Crystals, Molecular Crystals and Liquid Crystals, 74:1, 89-108

To link to this article: http://dx.doi.org/10.1080/00268948108073696

Mol. Cryst. Liq. Cryst., 1981, Vol. 74, pp. 89–108
0026-8941/81/7404-0089 $06.50/0

Printed in the United States of America

The Search for Quantum Liquid Crystals†‡

SUJANE C. WANG, § LEGESSE SENBETU and CHIA-WEI WOO

Department of Physics, University of California, San Diego
La Jolla, California 92093, U.S.A.

(*Received July 22, 1980*)

We report here our progress in the search for quantum liquid crystals. By "quantum liquid crystals," we mean quantum liquids which exhibit macroscopic orientational order but no (or incomplete) spatial order. Such a system is necessarily composed of light molecules, so that even at very low temperatures the zero-point motion of the molecules keeps the system in the liquid state. The molecules must be sufficiently anisotropic and the interactions sufficiently orientation-dependent to bring about macroscopic orientational order under appropriate conditions. Our goal is to identify such systems and predict the conditions under which liquid crystalline phases can occur.

The most natural candidate is ortho-hydrogen. Despite the light mass of the molecules, the strong intermolecular attraction forces the system at low temperature into a crystal in free space. To prevent this from happening, we introduce an external field which makes it energetically advantageous to keep the molecules well apart, by means of an adsorbing substrate such as a graphite surface. At zero temperature and varying areal densities, at least the following two-dimensional phases are possible: lattice gas, liquid and Debye-solid phases incommensurate with the surface symmetry of graphite each with or without orientational order, and superlattices (structures which are commensurate with graphite) with overlayer(s). The factors that determine whether among this rich variety of phases one or more liquid crystalline phases would stand out as the most stable now include the orientation-dependent molecule-substrate interaction, putting the theoretical problem at the crossroads of surface physics, low temperature physics, quantum many body problem, and phase transitions.

We employ for the variational wavefunction a highly correlated Feenberg (Jastrow) function:

$$\Psi(1,\ldots,N)=\prod_{i=1}^{N}\varphi(\mathbf{r}_i,\hat{\Omega}_i)\prod_{j>k=1}^{N}f(r_{jk},\hat{\Omega}_j,\hat{\Omega}_k).$$

$\varphi(\mathbf{r}_i,\hat{\Omega}_i)$ contains a laterally periodic function, $t(\rho_i,\hat{\Omega}_i)$ expanded in the reciprocal lattice space as

$$\sum_{\mathbf{G}}\sum_{l,m}t_{\mathbf{G}}^{2l,m}\exp(i\mathbf{G}\cdot\rho_i)\,Y_{2l}^{m}(\hat{\Omega}_i)$$

---

† Presented at the Eighth International Liquid Crystal Conference, Kyoto, July 1980.

‡ Work supported in part by the U.S. National Science Foundation under Grant No. DMR 80-08816.

§ Ph.D. candidate at Northwestern University.

permitting descriptions of all two-dimensional structures, including the liquid phases—in the limit $G \to 0$. We separate z from ρ and $\hat{\Omega}$ as a simplifying approximation. In the evaluation of the energy expectation value $\langle H \rangle$, the full Hamiltonian used includes a periodic hydrogen-substrate potential and a realistic hydrogen–hydrogen potential. One- and two-particle correlation functions, $P^{(1)}(\mathbf{r}, \hat{\Omega})$ and $P^{(2)}(\mathbf{r}_1, \hat{\Omega}_1, \mathbf{r}_2, \hat{\Omega}_2)$, are obtained from coupled integral equations, and then entered into the expression for $\langle H \rangle$. $P^{(1)}(\mathbf{r}, \hat{\Omega})$ carries information on the macroscopic order of the system (while $P^{(2)}$ describes short-range correlations). If several solutions for $P^{(1)}$ exist, $\langle H \rangle$ must be evaluated for each. From comparison we then determine which phase is stable in the statistical sense.

I INTRODUCTION

What is a quantum liquid crystal?

A liquid crystal represents a condensed phase of matter which displays macroscopic orientational order but incomplete (or no) macroscopic spatial order. At a fixed density, as the temperature is lowered, a system made up of anisotropic molecules can undergo transitions from an isotropic liquid phase to a liquid crystalline phase, and then from one or a series of liquid crystalline phases to a crystalline phase. The transitions can also take place at a fixed temperature as a consequence of varying the density.

In searching for a *quantum* liquid crystal, we choose temperatures which are very low, so as to accentuate the quantum effects. In the ideal case, we work (theoretically) with zero temperature and look for phase transitions as density varies. The requirements for a *quantum* mesophase to occur are as follows:

(i) The molecules must be anisotropic, so that an orientational axis can be defined.

(ii) The molecules must be sufficiently light and their moments of inertia sufficiently small to permit significant zero point motion, both translational and rotational.

(iii) The intermolecular force must have an orientational dependence as well as a spatial dependence.

There is a competition between (ii) and (iii). If the zero point motion cannot overcome the ordering effects of the intermolecular force, the system will have frozen into an orientationally ordered crystal. There is also competition between the orientational and the spatial components of the interaction. Depending on the outcome of the competition, the resulting mesophase can be a quantum plastic crystal or a quantum liquid crystal.

What substances will make the best candidates for our search? The lightest molecule that one can find is hydrogen. Being diatomic, the hydrogen molecule *can* be anisotropic; while para-hydrogen is spherically symmetric, ortho-hydrogen is not. The intermolecular potential has both orientational and spatial dependences. All three conditions are thus satisfied. However, the spatial component of the interaction dominates. The molecular solid that results is a face-centered cubic composed of four superimposed, orientationally ordered, simple cubic lattices. There is no quantum liquid crystalline phase.

The next candidate is helium. Helium molecules are light, and the spatial interaction is weak. Even at zero degree the system remains a liquid, thus a *quantum* liquid. But helium molecules are spherically symmetric. The isotope ^{3}He does have another degree of freedom: the spin. Spin–spin interaction, not unlike orientation-dependent forces, *can* lead to spin ordering in liquid ^{3}He, but it cannot be referred to as a quantum liquid crystal.

All other molecules are too heavy to exhibit zero point effects, and so we return to ortho-hydrogen. Some mechanism need be found to weaken the dominance of the spatial attraction between molecules. The presence of a moderating medium can do that. So we come upon physically adsorbed monolayers of ortho-hydrogen—in particular, ortho-hydrogen adsorbed on a graphite substrate.

The graphite surface is hexagonal in structure. Each hexagon provides an adsorption site. The sites make up a triangular lattice. However, each site is too small to contain a hydrogen molecule, so the substrate cannot sustain a close-packed two-dimensional crystal. At areal densities smaller than the density of adsorption sites, hydrogen molecules cannot cluster in neighboring sites. Thus they form a lattice gas, or a two-dimensional liquid, except at densities commensurate with the lattice of adsorption sites, e.g. at coverages corresponding to one-third or one-fourth the density of lattice sites. Molecules in liquids described here will show preferences for residing in or near adsorption sites. In other words, the density distribution will not be totally constant. Rather, there will be mild peaks at adsorption sites and valleys at adsorption ridges. But since the peaks will be too broad to imply localization of molecules, the system will still be in the liquid phase.

Some work has already been done on ortho-hydrogen physisorbed on graphite. In 1978, Berlinsky and Harris[1] studied the mean field theory of hydrogen fixed on lattice sites of a $\frac{1}{3}$-coverage superlattice. The substrate was considered as providing an anisotropic crystal field, and the molecules were correlated to one another via an electrostatic quadrupole–quadrupole interaction. At zero temperature, it was predicted that the system would undergo transitions to several orientationally ordered phases. Starting with a finite temperature, it was predicted that as the system cools there would also be transitions to orientationally ordered phases made up of sublattices. In 1979, O'Shea and Klein[2] reported on the results of a Monte Carlo calculation. Again, with the molecules fixed on lattice sites, a planar model (which limits the orientations and all rotations to a plane parallel to the adsorbing surface) would call for a transition temperature of 1.5 K, whereas a freely rotating three-dimensional model would make its transition at 1.0 K. Both theoretical calculations assumed fixed crystalline lattices, and both thus disregarded zero point effects. We do not feel that the resulting predictions are reliable. There was certainly no attempt toward finding a ***quantum liquid*** crystalline phase.

Also in 1978, Kubik and Hardy[3] probed the orientational behavior of hydrogen molecules physisorbed on graphite experimentally using NMR technique. The authors found the substrate field weak, and no orientational order was observed down to 1.3 K.

In this work, we conduct a search for orientational order in a realistic model of ortho-hydrogen physisorbed on graphite. Since we have in the past done quantum-mechanical calculations for helium[4] and para-hydrogen[5] adsorbed on graphite, and in particular we have accumulated much experience at densities around $\frac{1}{3}$-coverage, we carry out our preliminary calculation at $\frac{1}{3}$-coverage. The calculation makes use of quantum many body variational techniques developed by us in earlier work on transitions between quantum phases.[6] It goes beyond Hartree theory—quantum version of the mean field theory, and takes into account (spatial) correlations between molecules.

Section II reviews our quantum variational theory, by looking at para-hydrogen physisorbed on graphite. The formalism is mathematically simpler since orientation does not play a role. Section III outlines the formalism for ortho-hydrogen. Section IV summarizes results up to this point, and discusses conditions under which quantum liquid crystals can exist. Limitations of computer time prevented us from reaching firm conclusions at this time, but some directions have been identified, and further numerical work is in progress.

II PARA-HYDROGEN SUPERLATTICE

Our interest is in studying orientational ordering in a physically adsorbed monolayer of anisotropic molecules, e.g. ortho-hydrogen on graphite. However, let us review first the theory of spatial ordering in an adsorbed monolayer of *isotropic* molecules—in particular, para-hydrogen on a graphite surface at low coverages. The review will lay the groundwork for the quantum mechanical problem, and make the remaining parts of the paper more readable to those who are not familiar with quantum many body theory.

We consider a system of N para-hydrogen molecules in the neighborhood of a graphite surface of area A. The areal density is then $n \equiv N/A$. The surface structure is hexagonal, and gives rise to adsorption sites in the form of a triangular lattice. We choose the coordinate system as follows. Let the semi-infinite graphite substrate fill the lower half-space $z \leq 0$, the $z = 0$ plane coinciding with the substrate surface. Let the origin fall on one of the adsorption sites. The i-th hydrogen molecule, at position $\mathbf{r}_i$ above the graphite surface, interacts with each of the substrate molecules. As a result, it finds itself under the influence of a substrate potential $U(\mathbf{r}_i)$, which has a deep and narrow minimum when plotted against z_i. This potential confines the molecule near the substrate surface, and subjects it to a periodic potential along the xy-plane.

The Hamiltonian of the system can be written as

$$H = \sum_{i=1}^{N} - \frac{\hbar^2}{2M} \nabla_i^2 + \sum_{i<j=1}^{N} v(\mathbf{r}_{ij}) + \sum_{i=1}^{N} U(\mathbf{r}_i), \tag{1}$$

where M stands for the mass of a hydrogen molecule, and $v(\mathbf{r}_{ij})$ represents the hydrogen–hydrogen interaction, which is central in the case of para-hydrogen. The quantum mechanical ground-state problem consists of determining a good approximate wave function with the proper exchange symmetry. In the variational approach, it means the determination—from a set of trial wave functions—one that minimizes the energy expectation value. The spatial symmetry of this optimum wave function will reveal the spatial structure, or phase, of the system.

In choosing trial wave functions, it is crucial to take into account the essential physical features of the system. In the independent particle model, one would solve the single particle equation

$$\left[- \frac{\hbar^2}{2M} \nabla^2 + U(\mathbf{r}) \right] \xi(\mathbf{r}) = e_0 \xi(\mathbf{r}) \tag{2}$$

for the ground state $\xi(\mathbf{r})$, and form a symmetrized product $\prod_{i=1}^{N} \xi(\mathbf{r}_i)$ to account for the Bose statistics. But when pairwise interactions are non-negligible, the wave function must be modified to take into consideration pair correlations. For example, correlating factors $f(r_{ij})$, which die off rapidly when r_{ij} becomes comparable to the molecular diameter, should be introduced to prevent overlap of molecules. Otherwise the energy expectation value would diverge. Wave functions of such correlated forms are known as Feenberg-Jastrow functions:

$$\psi(\mathbf{r}_1, \mathbf{r}_2, \ldots, \mathbf{r}_N) = \prod_{i=1}^{N} \varphi(\mathbf{r}_i) \prod_{j<k=1}^{N} \exp[\tfrac{1}{2} U(r_{jk})], \tag{3}$$

where $\varphi(\mathbf{r})$ represents single particle functions which resemble $\xi(\mathbf{r})$, and $f(r_{jk})$ has been written as $\exp[\frac{1}{2} u(r_{jk})]$ for convenience, without loss of generality. The energy expectation value

$$E \equiv \frac{<\psi | H | \psi>}{<\psi | \psi>} \tag{4}$$

is then to be minimized with respect to variational parameters built into $\varphi(\mathbf{r})$ and $u(r)$.

At low areal densities, motions in the xy-plane are not strongly coupled to motions in the z direction. The mathematics can be simplified tremendously by taking

$$\varphi(\mathbf{r}) = \exp[\tfrac{1}{2}t(\rho)]x(z), \tag{5}$$

where

$$t(\rho) = \sum_{\mathbf{G}} t_{\mathbf{G}} \exp(i\mathbf{G}\cdot\rho). \tag{6}$$

ρ denotes the two-dimensional vector (x,y) and $\{\mathbf{G}\}$ the complete set of two-dimensional reciprocal lattice vectors corresponding to a chosen lattice structure. $x(z)$ can, for example, be taken as the ground state wave function of a molecule in the laterally averaged substrate potential $\bar{U}(z)$. The only variable parameters are then the expansion coefficients $\{t_{\mathbf{G}}\}$. Note that, first of all, the wave function described by Eqs. (3), (5), and (6) is properly symmetrized with respect to exchange. And second, it is equally valid for the liquid phase and every solid phase. When the energy minimum occurs at $t_{\mathbf{G}} = 0$ for all $\mathbf{G}$, the wave function has the symmetry of a liquid. Otherwise it will have the symmetry of a solid: a symmetry that inverts to $\{\mathbf{G}\}$.

The energy expectation value is given by

$$E = \int P^{(1)}(\mathbf{r}_1)\left\{-\frac{\hbar^2}{2M}\left[\frac{1}{2}\nabla^2_{\rho_1}t(\rho_1) + \frac{\partial^2}{\partial Z_1^2}\ln x(z_1)\right] + U(\mathbf{r}_1)\right\}d\mathbf{r}_1$$

$$+\frac{1}{2}\int P^{(2)}(\mathbf{r}_1,\mathbf{r}_2)\left[-\frac{\hbar^2}{4M}\nabla_1^2 u(r_{12}) + v(\mathbf{r}_{12})\right]d\mathbf{r}_1 d\mathbf{r}_2 \tag{7}$$

where $P^{(1)}(\mathbf{r}_1)$ and $P^{(2)}(\mathbf{r}_1,\mathbf{r}_2)$ are the one- and two-particle distribution functions defined by the general formula

$$P^{(n)}(\mathbf{r}_1,\mathbf{r}_2,\ldots,\mathbf{r}_n) = \frac{N!}{(N-n)!}\frac{\int |\psi|^2 d\mathbf{r}_{n+1}\ldots d\mathbf{r}_N}{\int |\psi|^2 d\mathbf{r}_1\ldots d\mathbf{r}_N}. \tag{8}$$

Since the molecules are confined to a very thin layer of space (nearly a planar region), especially when the areal densities are low, the lateral correlations dominate. One might approximate $v(r)$ by $v(\rho)$, $u(r)$ by $u(\rho)$, and correspondingly, $P^{(1)}$ and $P^{(2)}$ by

$$P^{(1)}(\mathbf{r}_1) \approx P^{(1)}(\rho_1)x^2(z_1), \tag{9}$$

and

$$P^{(2)}(\mathbf{r}_1,\mathbf{r}_2) \approx P^{(2)}(\rho_1,\rho_2)x^2(z_1)x^2(z_2)$$
$$\equiv P^{(1)}(\rho_1)P^{(1)}(\rho_2)g(\rho_1,\rho_2)x^2(z_1)x^2(z_2) \quad (10)$$

For every choice of the trial wave function, the task of evaluating E reduces then to a determination of $P^{(1)}(\rho_1)$ and $g(\rho_1,\rho_2)$.

One way of calculating $P^{(1)}(\rho_1)$ and $g(\rho_1,\rho_2)$ is to obtain generalized Bogoliubov-Born-Green-Kirkwood-Yvon (BBGKY) equations by taking the gradients of $P^{(1)}$ and $P^{(2)}$, introducing the definition of $P^{(3)}(\rho_1,\rho_2,\rho_3)$, and approximating the latter by use of a Kirkwood superposition approximation (KSA):

$$P^{(3)}(\rho_1,\rho_2,\rho_3) \approx P^{(1)}(\rho_1)P^{(1)}(\rho_2)P^{(1)}(\rho_3)g(\rho_1,\rho_2)g(\rho_2,\rho_3)g(\rho_3,\rho_1) \quad (11)$$

We find:

$$\nabla_{\rho_1}P^{(1)}(\rho_1) = P^{(1)}(\rho_1)\nabla_{\rho_1}t(\rho_1)$$
$$+ P^{(1)}(\rho_1)\int P^{(1)}(\rho_2)g(\rho_1,\rho_2)\nabla_{\rho_1}u(\rho_{12})d\rho_2, \quad (12)$$

and

$$\nabla_{\rho_1}\ln g(\rho_1,\rho_2) = \nabla_{\rho_1}u(\rho_{12})$$
$$+\int P^{(1)}(\rho_3)g(\rho_1,\rho_3)[g(\rho_2,\rho_3)-1]\nabla_{\rho_1}u(\rho_{13})d\rho_3 \quad (13)$$

Solving these coupled equations is no trivial matter. Often we have to resort to further approximations such as solving Eq. (13) for a liquid-like $P^{(1)}(\rho_3)$ and using the resulting liquid-like $g(\rho_1,\rho_2) \equiv g(\rho_{12})$ in Eq. (12). In that case, it is both convenient and physically revealing to write

$$P^{(1)}(\rho) = n\sum_{\mathbf{G}} a_{\mathrm{G}}\exp(i\mathbf{G}\cdot\rho) \quad (14)$$

and cast Eq. (12) in for form:

$$a_{\mathrm{G}} = \frac{1}{G}\sum_{\mathrm{G}'\neq 0} a_{\mathrm{G}-\mathrm{G}'}\hat{G}\cdot\hat{G}'[G't_{\mathrm{G}'} + na_{\mathrm{G}'}F(G')], \quad (15)$$

with

$$F(G') = -2\pi\int_0^\infty \rho g(\rho)u'(\rho)J_1(G'\rho)d\rho. \quad (16)$$

$\{a_{\mathrm{G}}\}$ can be obtained by iterating Eq. (15). They provide us with an analysis of $P^{(1)}(\rho)$, and thus a direct description of the density distribution.

In such calculations, the choice of the correlating element $u(\rho_{jk})$ can be quite crucial. For Lennard-Jones potentials $v(r)$, we were taught by experience to use the form

$$u(\rho) = -\left(\frac{a}{\rho}\right)^m \tag{17}$$

where a and m are variational parameters.

In a recent paper,[5] we applied the above theory to the ground state of para-hydrogen monolayers physically adsorbed on a graphite surface. We found that at $\frac{1}{3}$-coverage, i.e., areal density corresponding to having one-third of the adsorption sites occupied, a triangular superlattice turns out to be the stable phase. At $\frac{1}{4}$-coverage, however, the superlattice phase is unstable against transition to a two-dimension liquid phase.

III ORTHO-HYDROGEN ADSORBED ON GRAPHITE

Ortho-hydrogen molecules are not spherically symmetric. The coordinates of an ortho-hydrogen molecule consists of the position of its center of mass $\mathbf{r}_i$, and the orientation of its internuclear axis, $\hat{\Omega}_i$. For a set of N such molecules in the neighborhood of the same graphite surface as described in the last section, the Hamiltonian becomes

$$H = \sum_{i=1}^{N}\left(-\frac{\hbar^2}{2M}\nabla_i^2 + \frac{\hbar^2}{2I}J_i^2\right) + \sum_{i>j=1}^{N} v(\mathbf{r}_{ij},\hat{\Omega}_i,\hat{\Omega}_j) + \sum_{i=1}^{N} U(\mathbf{r}_i,\hat{\Omega}_i), \tag{18}$$

where I is the moment of inertia of the molecule, and J_i^2 denotes the angular momentum operator. Note that both the hydrogen–hydrogen interaction and the hydrogen–substrate interaction depend now on the molecular orientations.

Following the previous prescription, the trial wave function for such a system can be written in the form

$$\psi(\mathbf{r}_1,\hat{\Omega}_1,\mathbf{r}_2,\hat{\Omega}_2,\ldots,\mathbf{r}_N,\hat{\Omega}_N) = \prod_{i=1}^{N}\varphi(\mathbf{r}_i,\hat{\Omega}_i)\prod_{j>k=1}^{N}\exp[\tfrac{1}{2}u(\mathbf{r}_{jk},\hat{\Omega}_j,\hat{\Omega}_k)]. \tag{19}$$

We can write

$$\varphi(\mathbf{r},\hat{\Omega}) = \exp[\tfrac{1}{2}t(\rho,\hat{\Omega})]x(z), \tag{20}$$

with

$$t(\rho,\hat{\Omega}) = \sum_{\mathbf{G}}\sum_{l,m} t_{\mathbf{G}}^{2l,m}\exp(i\mathbf{G}\cdot\rho)\,Y_{2l}^{m}(\hat{\Omega}), \tag{21}$$

at areal densities low enough to permit the decoupling of motions in the xy-plane from that in the z-direction. On account of the homonuclear property of the hydrogen molecule, only even-l terms need be retained in the expansion formula. The coefficients $\{t_G^{2l,m}\}$ are now the variational parameters. They will determine whether the system is in the two-dimensional liquid or solid phase, and how the molecules are oriented.

By the same argument as in the previous section, we approximate $v(\mathbf{r}_{ij}, \hat{\Omega}_i, \hat{\Omega}_j)$ and $u(r_{ij}, \hat{\Omega}_i, \hat{\Omega}_j)$ by $v(\rho_{ij}, \hat{\Omega}_i, \hat{\Omega}_j)$ and $u(\rho_{ij}, \hat{\Omega}_i, \hat{\Omega}_j)$, respectively. $u(\rho_{ij}, \hat{\Omega}_i, \hat{\Omega}_j)$ will be parameterized thus:

$$u(\rho_{ij}, \hat{\Omega}_i, \hat{\Omega}_j) = -\left(\frac{a}{\rho_{ij}}\right)^m [1 + \alpha P_2(\hat{\Omega}_i \cdot \hat{\Omega}_j)] \equiv u(\rho_{ij}) y(\hat{\Omega}_i, \hat{\Omega}_j), \tag{22}$$

where a, m, and α are variational parameters. At low areal densities, the anisotropic effects are not strong; one can take a and m to be the same as for para-hydrogen. So there is only one new variational parameter in the correlating element: α. α is expected to be small.

The energy expression becomes

$$\begin{aligned}
E &\equiv \frac{\langle \psi | H | \psi \rangle}{\langle \psi | \psi \rangle} \\
&= \int P^{(1)}(\mathbf{r}_1, \hat{\Omega}_1) \left[-\frac{\hbar^2}{4M} \nabla_1^2 \ln \varphi(\mathbf{r}_1, \hat{\Omega}_1) + \frac{\hbar^2}{2I} \frac{1}{\varphi(\mathbf{r}_1, \hat{\Omega}_1)} J_1^2 \varphi(\mathbf{r}_1, \hat{\Omega}_1) \right. \\
&\quad \left. + U(\mathbf{r}_1, \hat{\Omega}_1) \right] d\mathbf{r}_1 d\hat{\Omega}_1 \\
&\quad + \frac{1}{2} \int P^{(2)}(\mathbf{r}_1, \hat{\Omega}_1, \mathbf{r}_2, \hat{\Omega}_2) \left\{ -\frac{\hbar^2}{4M} \nabla_{\rho_1}^2 u(\rho_{12}, \hat{\Omega}_1, \hat{\Omega}_2) \right. \\
&\quad + \frac{\hbar^2}{I} \exp\left[-\frac{1}{2} u(\rho_{12}, \hat{\Omega}_1, \hat{\Omega}_2) \right] J_1^2 \exp\left[\frac{1}{2} u(\rho_{12}, \hat{\Omega}_1, \hat{\Omega}_2) \right] \\
&\quad \left. + v(\rho_{12}, \hat{\Omega}_1, \hat{\Omega}_2) \right\} d\mathbf{r}_1 d\hat{\Omega}_1 d\mathbf{r}_2 d\hat{\Omega}_2,
\end{aligned} \tag{23}$$

where $P^{(1)}(\mathbf{r}_1, \hat{\Omega}_1)$ and $P^{(2)}(\mathbf{r}_1, \hat{\Omega}_1, \mathbf{r}_2, \hat{\Omega}_2)$ are generalized one- and two-particle distribution functions defined by

$$\begin{aligned}
&P^{(n)}(\mathbf{r}_1, \hat{\Omega}_1, \mathbf{r}_2, \hat{\Omega}_2, \ldots, \mathbf{r}_n, \hat{\Omega}_n) \\
&\qquad = \frac{N!}{(N-n)!} \frac{\int |\psi|^2 d\mathbf{r}_{n+1} d\hat{\Omega}_{n+1} \ldots d\mathbf{r}_N d\hat{\Omega}_N}{\int |\psi|^2 d\mathbf{r}_1 d\hat{\Omega}_1 \ldots d\mathbf{r}_N d\hat{\Omega}_N}
\end{aligned} \tag{24}$$

We take as before

$$P^{(1)}(\mathbf{r}_1,\hat{\Omega}_1) \to P^{(1)}(\rho_1,\hat{\Omega}_1)x^2(z_1) \tag{25}$$

and

$$\begin{aligned} P^{(2)}(\mathbf{r}_1,\hat{\Omega}_1,\mathbf{r}_2,\hat{\Omega}_2) &\to P^{(2)}(\rho_1,\hat{\Omega}_1,\rho_2,\hat{\Omega}_2)x^2(z_1)x^2(z_2) \\ &\equiv P^{(1)}(\rho_1,\hat{\Omega}_1)P^{(1)}(\rho_2,\hat{\Omega}_2)g(\rho_1,\hat{\Omega}_1,\rho_2,\hat{\Omega}_2)x^2(z_1)x^2(z_2) \end{aligned} \tag{26}$$

Further, we let

$$\begin{aligned} g(\rho_1,\hat{\Omega}_1,\rho_2,\hat{\Omega}_2) \approx g(\rho_{12},\hat{\Omega}_1\cdot\hat{\Omega}_2) &= \sum_{l=0}^{\infty} g_{2l}(\rho_{12})P_{2l}(\hat{\Omega}_1\cdot\hat{\Omega}_2) \\ &\approx g_0(\rho_{12}) + g_2(\rho_{12})P_2(\hat{\Omega}_1\cdot\hat{\Omega}_2) \end{aligned} \tag{27}$$

The truncated form is expected to make a good approximation at low areal densities

Differentiating $P^{(1)}(\rho_1,\hat{\Omega}_1)$ with the operators ∇_{ρ_1} and $\mathbf{J}_1$, we find

$$\begin{aligned} \nabla_{\rho_1}P^{(1)}(\rho_1,\hat{\Omega}_1) &= P^{(1)}(\rho_1,\hat{\Omega}_1)\nabla_{\rho_1}t(\rho_1,\hat{\Omega}_1) \\ &+ P^{(1)}(\rho_1,\hat{\Omega}_1)\int P^{(1)}(\rho_2,\hat{\Omega}_2)g(\rho_{12},\hat{\Omega}_1\cdot\hat{\Omega}_2)y(\hat{\Omega}_1\cdot\hat{\Omega}_2)\nabla_{\rho_1}u(\rho_{12})d\rho_2 d\hat{\Omega}_2 \end{aligned} \tag{28}$$

and

$$\begin{aligned} \mathbf{J}_1P^{(1)}(\rho_1,\hat{\Omega}_1) &= P^{(1)}(\rho_1,\hat{\Omega}_1)\mathbf{J}_1 t(\rho_1,\hat{\Omega}_1) \\ &+ \alpha P^{(1)}(\rho_1,\hat{\Omega}_1)\int P^{(1)}(\rho_2,\hat{\Omega}_2)g(\rho_{12},\hat{\Omega}_1\cdot\hat{\Omega}_2)u(\rho_{12})\mathbf{J}_1P_2(\hat{\Omega}_1\cdot\hat{\Omega}_2)d\rho_2 d\hat{\Omega}_2. \end{aligned} \tag{29}$$

Differentiating $P^{(2)}(\rho_1,\hat{\Omega}_1,\rho_2,\hat{\Omega}_2)$ with the operators ∇_{ρ_1} and J_{1z}, and using the generalized KSA

$$\begin{aligned} P^{(3)}(\rho_1,\hat{\Omega}_1,\rho_2,\hat{\Omega}_2,\rho_3,\hat{\Omega}_3) &\approx P^{(1)}(\rho_1,\hat{\Omega}_1)P^{(1)}(\rho_2,\hat{\Omega}_2)P^{(1)}(\rho_3,\hat{\Omega}_3) \\ &\quad g(\rho_{12},\hat{\Omega}_1\cdot\hat{\Omega}_2)g(\rho_{23},\hat{\Omega}_2\cdot\hat{\Omega}_3)g(\rho_{31},\hat{\Omega}_3\cdot\hat{\Omega}_1), \end{aligned} \tag{30}$$

we obtain for $g_2(\rho) \ll g_0(\rho)$ the coupled equations

$$\begin{aligned} \frac{\partial}{\partial\rho_{12}}[\ln g_0(\rho_{12})] &= \frac{\partial u(\rho_{12})}{\partial\rho_{12}} \\ &+ \int(\hat{\rho}_{12}\cdot\hat{\rho}_{13})\left[\frac{\partial u(\rho_{13})}{\partial\rho_{13}}\right]P^{(1)}(\rho_3,\hat{\Omega}_3)[g_0(\rho_{23})-1] \\ &\qquad \left[g_0(\rho_{13}) + \frac{\alpha}{5}g_2(\rho_{13})\right]d\rho_3 d\hat{\Omega}_3, \end{aligned} \tag{31}$$

and

$$\frac{g_2(\rho_{12})}{g_0(\rho_{12})} = \alpha u(\rho_{12}) + \frac{4\pi\alpha}{5}\int u(\rho_{13}) P^{(1)}(\boldsymbol{\rho}_3, \hat{\Omega}_3) g_2(\rho_{23}) g_0(\rho_{13}) Y_2^{*1}(\hat{\Omega}_3) Y_2^1(\hat{\Omega}_3) d\boldsymbol{\rho}_3 d\hat{\Omega}_3. \quad (32)$$

The entire problem reduces to the solution of Eqs. (28), (29), (31) and (32) for $P^{(1)}(\boldsymbol{\rho}_1, \hat{\Omega}_1)$, $g_0(\rho_{12})$, and $g_2(\rho_{12})$, given a set of values for the variational parameters $\{t_{\mathrm{G}}^{2l,m}\}$ and α.

The solution for $P^{(1)}(\boldsymbol{\rho}, \hat{\Omega})$ is further facilitated by the expansion

$$P^{(1)}(\boldsymbol{\rho}, \hat{\Omega}) = n \sum_{\mathrm{G}} \sum_{l,m} a_{\mathrm{G}}^{2l,m} \exp(i\mathrm{G}\cdot\boldsymbol{\rho}) Y_{2l}^{m}(\hat{\Omega}), \quad (33)$$

where the coefficients $\{a_{\mathrm{G}}^{2l,m}\}$ can be determined iteratively for given $g_0(\rho_{12})$ and $g_2(\rho_{12})$. The solution for $g_0(\rho_{12})$ and $g_2(\rho_{12})$ can in turn be obtained for given $P^{(1)}(\boldsymbol{\rho}, \hat{\Omega})$. The latter is difficult to achieve except in the case of a liquid-like $P^{(1)}(\boldsymbol{\rho}, \hat{\Omega})$. We make that approximation in the preliminary numerical calculation reported here. Further, as long as α is small, $g_0(\rho)$ will not deviate much from the $g(\rho)$ obtained from the para-hydrogen calculation. We make that assumption here, and later demonstrate numerically that α is indeed small in all cases of interest. Thus, only Eq. (32) need be solved, and only for $P^{(1)}(\boldsymbol{\rho}, \hat{\Omega}) = n$.

IV NUMERICAL WORK, RESULTS, AND DISCUSSIONS

In actual calculation we need to specify the hydrogen–hydrogen interaction $v(\rho_{12}, \hat{\Omega}_1, \hat{\Omega}_2)$ and the hydrogen–substrate potential $U(\mathbf{r}, \hat{\Omega})$. For the former, we employ the form given by Etters *et al.*,[10] which includes both short-range valence interaction and long-range multipole terms. The formulas are reproduced in the Appendix. For the latter, we begin with a parameterized hydrogen–carbon potential:

$$e(R, \Theta) = 4\epsilon\left[\left(\frac{\sigma}{R}\right)^{12} - \left(\frac{\sigma}{R}\right)^{6}\right] + 4\epsilon\left[b'\left(\frac{\sigma}{R}\right)^{12} - c'\left(\frac{\sigma}{R}\right)^{6}\right] P_2(\cos\Theta), \quad (34)$$

where $\mathbf{R}$ denotes the (vector) separation between the center of mass of the hydrogen molecule and that of the carbon atom, and Θ the angle between $\mathbf{R}$ and the molecular axis of hydrogen. (ϵ, σ) and (b', c') are two pairs of adjustable parameters to be determined empirically. $U(\mathbf{r}, \hat{\Omega})$ comes, then, from summing $e(R, \Theta)$ over the entire carbon substrate lattice.

At the present time, the determination of (ϵ, σ) and (b', c') is an art. An ideal calculation would be to use the scattering data of ortho-hydrogen against a graphite surface to fit the eigenstates of $U(\mathbf{r}, \hat{\Omega})$, much like what was done for ^{4}He-graphite (-surface) interaction.[5,7] But good ortho-hydrogen-graphite (-surface) data are hard to come by. Using data on H_2 scattering against various molecules, we estimated the range of values for (b', c'). We were provided some preliminary data by G. Fletcher and co-workers,[8] and used them to estimate (ϵ, σ). The actual ortho-hydrogen-substrate potential used in our work is of the truncated form:

$$\begin{aligned} U(\mathbf{r}, \hat{\Omega}) &\equiv U(\rho, z; \theta, \varphi) = U_0(z) + U_2(z) P_2(\cos\theta) \\ &+ U_s(z)[\cos \mathbf{k}_1\cdot\rho + \cos \mathbf{k}_2\cdot\rho + \cos(\mathbf{k}_1+\mathbf{k}_2)\cdot\rho] + U_{2s}(z)[P_2(\cos\theta) - 1] \\ &\times \{\cos^2\varphi[\cos(\mathbf{k}_1+\mathbf{k}_2)\cdot\rho - \tfrac{1}{2}\cos \mathbf{k}_1\cdot\rho - \tfrac{1}{2}\cos \mathbf{k}_2\cdot\rho]\}, \end{aligned} \tag{35}$$

with

$$U_0(z) = \frac{4\pi\epsilon}{a_s} \sum_n \left(\frac{2}{5}\frac{\sigma^{12}}{z_n^{10}} - \frac{\sigma^6}{z_n^4}\right), \tag{36}$$

$z_n = z + nd$, d being the spacing between graphite layers,

$$U_2(z) = \frac{4\pi\epsilon}{a_s} \sum_n \left(\frac{\beta\sigma^{12}}{z_n^{10}} - \frac{\gamma\sigma^6}{z_n^4}\right), \tag{37}$$

$$\begin{aligned} &U_s(z) \\ &= -\frac{8\pi\epsilon}{a_s}\left[\frac{\sigma^{12}}{60}\left(\frac{2\pi}{\sqrt{3}a'z}\right)^5 K_5(kz) - \sigma^6\left(\frac{2\pi}{\sqrt{3}a'z}\right)^2 K_2(kz)\right], k \equiv |\mathbf{k}_1| \equiv |\mathbf{k}_2|, \end{aligned} \tag{38}$$

$$U_{2s}(z) = \frac{2\pi\epsilon}{3a_s}\left[\frac{\beta'\sigma^{12}}{z^4}\left(\frac{2\pi}{\sqrt{3}a'}\right)^6 K_4(kz) - \frac{\gamma'\sigma^6}{z}\left(\frac{2\pi}{\sqrt{3}a'}\right)^3 K_1(kz)\right], \tag{39}$$

where a_s is the area of a unit cell in the substrate, $\mathbf{k}_1$ and $\mathbf{k}_2$ are primitive vectors of the two-dimensional reciprocal lattice space corresponding to the graphite surface structure, a' is the distance between nearest neighbor adsorption sites, and K_l denotes the lth order Bessel function of the second kind.

β and γ are parameters related to b' and c'. We tried several sets of (β, γ) within the range of values bounded by experimental data. β' and γ' are also related to b' and c'. The spatial periodicity of the U_{2s} term is, however, such that it does not contribute to the energy. We thus make no further mention of β' and γ'.

The final expression of energy per molecule is:

$$E = E_1 + E_2 + E_3 + E_4 + E_5 + E_6, \tag{40}$$

where

$$E_1 \equiv \int P^{(1)}(\mathbf{r}_1, \hat{\Omega}_1)\left\{-\frac{\hbar^2}{4M}\left[\frac{1}{2}\nabla^2_{\rho_1} t(\rho_1, \hat{\Omega}_1) + \frac{d^2}{dz_1^2}\ln x(z_1)\right]\right\} d\mathbf{r}_1 d\hat{\Omega}_1, \tag{41}$$

$$E_2 \equiv \int P^{(1)}(\mathbf{r}_1, \hat{\Omega}_1)\,\frac{\hbar^2}{2I}\{\tfrac{1}{2}J_1^2 t(\rho_1, \hat{\Omega}_1) + \tfrac{1}{4}[(J_{1z}t(\rho_1, \hat{\Omega}_1))^2$$
$$+ (J_{1+}t(\rho_1, \hat{\Omega}_1))(J_{1-}t(\rho_1, \hat{\Omega}_1))]\} d\mathbf{r}_1 d\hat{\Omega}_1, \tag{42}$$

$$E_3 \equiv \int P^{(1)}(\mathbf{r}_1, \hat{\Omega}_1)\, U(\mathbf{r}_1, \hat{\Omega}_1) d\mathbf{r}_1 d\hat{\Omega}_1, \tag{43}$$

$$E_4 \equiv \int P^{(2)}(\mathbf{r}_1, \hat{\Omega}_1, \mathbf{r}_2, \hat{\Omega}_2)\left[-\frac{\hbar^2}{8M}\nabla^2_{\rho_1} u(\rho_{12}, \hat{\Omega}_1, \hat{\Omega}_2)\right] d\mathbf{r}_1 d\hat{\Omega}_1 d\mathbf{r}_2 d\hat{\Omega}_2, \tag{44}$$

$$E_5 \equiv \int P^{(2)}(\mathbf{r}_1, \hat{\Omega}_1, \mathbf{r}_2, \hat{\Omega}_2)\,\frac{\hbar^2}{4I}\Big\{J_1^2 u(\rho_{12}, \hat{\Omega}_1, \hat{\Omega}_2) + \frac{1}{2}[(J_{1z}u(\rho_{12}, \hat{\Omega}_1, \hat{\Omega}_2))^2$$
$$+ (J_{1+}u(\rho_{12}, \hat{\Omega}_1, \hat{\Omega}_2)(J_{1-}u(\rho_{12}, \hat{\Omega}_1, \hat{\Omega}_2))]\Big\} d\mathbf{r}_1 d\hat{\Omega}_1 d\mathbf{r}_2 d\hat{\Omega}_2, \tag{45}$$

$$E_6 \equiv \frac{1}{2}\int P^{(2)}(\mathbf{r}_1, \hat{\Omega}_1, \mathbf{r}_2, \hat{\Omega}_2) v(\rho_{12}, \hat{\Omega}_1, \hat{\Omega}_2) d\mathbf{r}_1 d\hat{\Omega}_1 d\mathbf{r}_2 d\hat{\Omega}_2. \tag{46}$$

Writing explicitly in terms of the expansion coefficients $\{t_{\mathrm{G}}^{2l,m}\}$ and $\{a_{\mathrm{G}}^{2l,m}\}$ and the pair correlation functions $g_0(\rho_{12})$ and $g_2(\rho_{12})$, Eqs. (41)–(46) become:

$$E_1 = \frac{\hbar^2}{8M}\sum_{\mathrm{G}}\sum_{l,m}(-1)^m a_{\mathrm{G}}^{2l,m} t_{-\mathrm{G}}^{2l,-m} G^2 + E_g - E_p, \tag{47}$$

where E_g is the energy of the state $x(z)$,

and

$$E_p = \begin{cases} \displaystyle\int x^2(z)\left[U_0(z) + \frac{h^2}{I} - \frac{1}{5}U_2(z)\right]dz, & \text{when } x(z) \text{ is the } m = \pm 1 \text{ eigenstate,} \\[2ex] \displaystyle\int x^2(z)\left[U_0(z) + \frac{h^2}{I} + \frac{2}{5}U_2(z)\right]dz, & \text{when } x(z) \text{ is the } m = 0 \text{ eigenstate,} \end{cases} \tag{48}$$

$$E_2 = \frac{\hbar^2}{4I} \sum_{\mathbf{G}} \sum_{l,m} (-1)^m 2l(2l+1) a_{\mathbf{G}}^{2l,m} t_{-\mathbf{G}}^{2l,-m}$$

$$+ \frac{1}{\sqrt{4}\pi} \frac{\hbar^2}{8I} \sum_{\mathbf{G}} \sum_{\mathbf{G}'} \Big\{ -6a_{\mathbf{G}}^{0,0}[2t_{\mathbf{G}'}^{2,2} t_{-(\mathbf{G}+\mathbf{G}')}^{2,-2} + 2t_{\mathbf{G}'}^{2,1} t_{(\mathbf{G}+\mathbf{G}')}^{2,1} + t_{\mathbf{G}'}^{2,0} t_{(\mathbf{G}+\mathbf{G}')}^{2,0}]$$

$$+ \frac{6\sqrt{5}}{7} a_{\mathbf{G}}^{2,2}[-\sqrt{6} t_{\mathbf{G}'}^{2,1} t_{-(\mathbf{G}'+\mathbf{G})}^{2,1} + 2t_{\mathbf{G}'}^{2,2} t_{-(\mathbf{G}+\mathbf{G}')}^{2,0} + 2t_{\mathbf{G}'}^{2,0} t_{-(\mathbf{G}+\mathbf{G}')}^{2,2}]$$

$$- \frac{6\sqrt{5}}{7} a_{\mathbf{G}}^{2,1}[\sqrt{6} t_{\mathbf{G}'}^{2,1} t_{-(\mathbf{G}'+\mathbf{G})}^{2,2} + t_{\mathbf{G}'}^{2,0} t_{-(\mathbf{G}'+\mathbf{G})}^{2,1} + 3t_{\mathbf{G}'}^{2,1} t_{-(\mathbf{G}'+\mathbf{G})}^{2,0}$$

$$+ t_{\mathbf{G}'}^{2,2} t_{-(\mathbf{G}'+\mathbf{G})}^{2,1}] + \frac{6\sqrt{5}}{7} a_{\mathbf{G}}^{2,0}[2t_{\mathbf{G}'}^{2,2} t_{-(\mathbf{G}+\mathbf{G}')}^{2,2} - 2t_{\mathbf{G}'}^{2,1} t_{-(\mathbf{G}'+\mathbf{G})}^{2,1}$$

$$- t_{\mathbf{G}'}^{2,0} t_{-(\mathbf{G}'+\mathbf{G})}^{2,0}] \Big\}, \quad (49)$$

$$E_3 = \int x^2(z) U_0(z) dz + a_0^{2,0} \sqrt{\frac{4\pi}{5}} \int U_2(z) x^2(z) dz$$

$$+ 3a_{\mathbf{G}}^{0,0} \sqrt{4\pi} \int x^2(z) U_s(z) dz, \quad (50)$$

$$E_4 = -n \frac{\pi^2 \hbar^2}{M} \sum_{\mathbf{G}} \Big\{ a_{\mathbf{G}}^{0,0} a_{-\mathbf{G}}^{0,0} \int \rho J_0(G\rho) g_0(\rho) \nabla_\rho^2 u_\rho(\rho) d\rho$$

$$+ \frac{1}{5} \sum_m (-1)^m a_{\mathbf{G}}^{2,m} a_{-\mathbf{G}}^{2,-m} \int \rho J_0(G\rho)[\alpha g_0(\rho) + g_2(\rho)] \nabla_\rho^2 u(\rho) d\rho \Big\}, \quad (51)$$

$$E_5 = \frac{\hbar^2}{2I} \frac{24}{5} \pi^2 \alpha n \sum_{\mathbf{G}} \Big\{ \sum_{m=-2}^{2} (-1)^m a_{\mathbf{G}}^{2,m} a_{-\mathbf{G}}^{2,-m} \int_0^\infty \rho J_0(G\rho) g_0(\rho) u(\rho) d\rho$$

$$+ \frac{1}{5} \int \rho J_0(G\rho) g_2(\rho) u(\rho) d\rho \Big[5a_{\mathbf{G}}^{0,0} a_{-\mathbf{G}}^{0,0}$$

$$+ \frac{10}{7} (2a_{\mathbf{G}}^{2,2} a_{-\mathbf{G}}^{2,-2} + 2a_{\mathbf{G}}^{2,1} a_{-\mathbf{G}}^{2,1} + a_{\mathbf{G}}^{2,0} a_{-\mathbf{G}}^{2,0}) \Big] \Big\}, \quad (52)$$

and E_6 gives the hydrogen–hydrogen interaction energy, which is straightforward to obtain, but too lengthy to be given here term-by-term.

In the numerical work reported here, we took four sets of the model parameters (β, γ). Case 1, (0.0672, 0.0585), gives a hydrogen-substrate potential that encourages the hydrogen molecules to lie *individually* in the plane of adsorption. The question is whether quantum and many body effects would cause them to stand up on the substrate surface. Case 2, (0.04, 0.06), gives a potential that encourages the hydrogen molecules to stand, ***individually;*** as do cases 3 and 4, (0.04, 0.045) and (0.045, 0.045) respectively, albeit weakly. The question is whether quantum and many body effects would cause them to lie down. By quantum effects, we refer to zero point motion, which tend to destroy order. By many body effects, we refer to the hydrogen-hydrogen correlation, which tends to make nearest-neighbors orient in normal directions with respect to each other.

For variational parameters, we have first of all α, which describes short-range orientational correlations. From Eq. (32), $\alpha = 0$ would result in $g_2(\rho) = 0$, giving rise to a radial pair distribution function. In the single-particle function $\varphi(\mathbf{r}, \hat{\Omega})$, we retain only the leading coefficients $t_{G_1}^{0,0}$, $t_0^{2,0}$, and $t_0^{2,2}$. We take $t_{G_1}^{0,0}$ to be the same as that for para-hydrogen at $\frac{1}{3}$-coverage. (Later work will vary this coefficient as well.) For convenience, we shall refer to $t_0^{2,0}$ as T_2 in the following, and $t_0^{2,0}$ as T_4. A finite T_2 indicates molecular orientations normal to the substrate surface, and a finite T_4 corresponds to molecular orientations parallel to the surface. α, T_2, and T_4 make up the set of variational parameters under consideration in our present work.

Tables I, II, III, and IV give energies as functions of α, T_2 and T_4. Table I lists energies at several sets of (T_2, T_4), each for a different α. One sees that in Case 1, the energy minimum occurs at $\alpha = 0.005$, $T_2 = 0$, and $T_4 = 0$. This means that, despite individual preferences for the molecules to orient parallel to the adsorbing surface, the system as a whole gives rise to *no* macroscopic orientation order. The quantum and many body effects require the system to be macroscopically isotropic. In Table II, we list only the energies about the minimum at $\alpha = 0.025$, $T_2 = 0.1$, and $T_4 = 0.0$. In this case the individual molecules prefer to orient normal to the surface. There remains a macroscopic orientational order in the normal direction, but a very weak one. In Tables III and IV, we list results for Cases 3 and 4, in which the individual molecules also prefer to orient normal to the surface, but barely so. The energy minimum corresponds to a random orientational configuration. Indications are that both the quantum and many body effects act to decrease the orientational order imposed on the system by the substrate potential. (There is some similarity between this case and the case of a classical *isotropic* nematogenic system placed under the influence of a strong orienting field.)

Figure 1 shows $g_2(\rho)$ for a set of α. A quick scan of Tables I–IV results in the conclusion that the α's that minimize the energies are all small, as expected. So, then, are the corresponding $g_2(\rho)$'s.

The restriction of computer time and the Conference deadline prevent us from obtaining more results at this time. Numerical computations are nonetheless continuing. We are studying cases involving other values of β and γ. It is reasonable to adjust these substrate parameters, partly because the hydrogen-carbon potential (and thus the substrate potential) is not well known, and

TABLE I

Energy as a function of T_2 and T_4 for $(\beta, \gamma) = (0.0672, 0.0585)$; (a) $\alpha = 0.1$, (b) $\alpha = 0.025$, (c) $\alpha = 0.005$, (d) $\alpha = -0.05$

	T_4 \ T_2	0.0	0.1	0.2
(a)	0.0	−374.69	−374.70	−374.42
	0.2	−374.16	−373.98	−373.62

	T_4 \ T_2	0.0	0.1	0.2
(b)	0.0	−375.98	−375.99	−375.55
	0.2	−374.94	−374.87	−374.62

	T_4 \ T_2	0.0	0.1	0.2
(c)	0.0	−376.14	−375.82	−375.39
	0.2	−375.15	−375.01	−374.68

	T_4 \ T_2	0.0	0.1	0.2
(d)	0.0	−375.23	−375.20	−374.72
	0.2	−374.31	−374.16	−373.69

TABLE II

Energy as a function of T_2 and T_4 for $\alpha = 0.025$ and $(\beta, \gamma) = (0.04, 0.06)$.

T_4 \ T_2	0.0	0.1	0.2
0.0	−372.98	−373.26	−373.09
0.1	−372.64	−372.85	−372.84
0.2	−371.93	−372.11	−372.13

TABLE III

Energy as a function of T_2 and T_4 for $\alpha = 0.005$ and $(\beta, \gamma) = (0.04, 0.045)$.

T_4 \ T_2	0.0	0.1	0.2
0.0	−372.35	−372.12	−371.79
0.1	−371.98	−371.84	−371.67
0.2	−371.33	−371.10	−371.07

TABLE IV

Energy as a function of T_2 and T_4 for $\alpha = 0.005$ and $(\beta, \gamma) = (0.045, 0.045)$.

T_4 \ T_2	0.0	0.1	0.2
0.0	−373.06	−372.77	−372.39
0.1	−372.69	−372.49	−372.27
0.2	−372.04	−371.75	−371.67

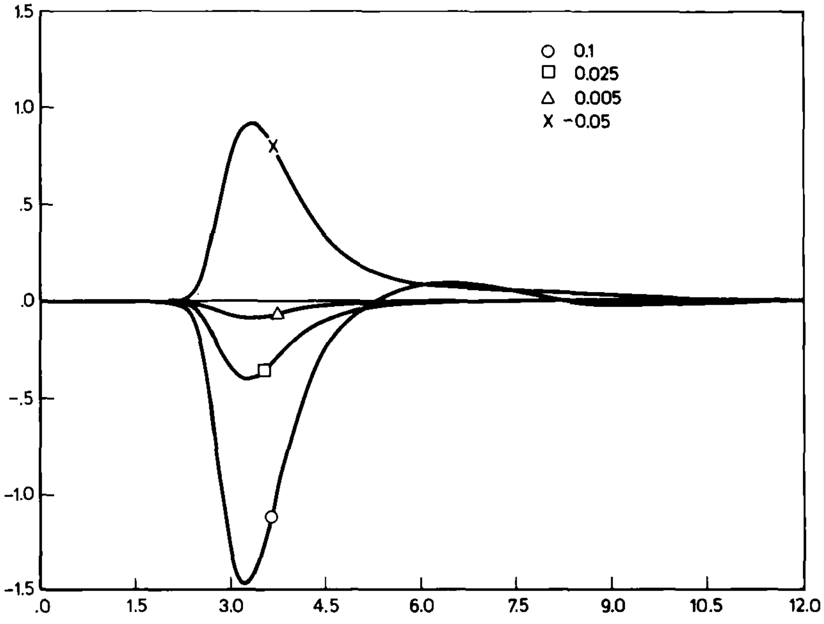

FIGURE 1 g_2 as a function of ρ for $\alpha = 0.1, 0.025, 0.005$ and -0.05.

partly because it is always possible, at least in principle, to prepare substrates other than graphite. We are also going toward lower areal densities than $\frac{1}{3}$-coverage while allowing $t_G^{0,0}$ to vary—to include the eventual onset of liquid phase before reaching $\frac{1}{4}$-coverage, where it is known that the superlattice structure is *not* stable. Our best hope is to find, at low coverages, nematic phases induced by the substrate potential—much like cases 2 and 3, but with energies minimized at $\{t_G^{0,0}\} = 0$, and at higher coverages, macroscopic isotropic phases with strong short range orientational ordering, i.e., interspersed orientationally ordered liquids or lattice gases with orthogonal directors.

What we have been able to show here is the varied interplays between quantum and correlation effects—the zero point motion, the H_2-H_2 correlation, and the H_2-substrate correlation. Out of these interplays come a rich variety of possible quantum phases of condensed matter. Problems such as this are most demanding in terms of experimental and theoretical techniques, but they are exciting because they bring together the subfields of low temperature physics, liquid crystal physics, and surface physics.

Acknowledgment

We are grateful to Dr. G. P. Felcher for sharing with us unpublished data on hydrogen scattered from graphite surfaces obtained by him and his collaborators. Also, we would like to thank Dr. D. C. Jou for valuable discussions.

Appendix

$$v(\mathbf{r}_{12}, \hat{\Omega}_1, \hat{\Omega}_2) = \sum_{i=1}^{8} A_i(r) B_i(r, \hat{\Omega}_1, \hat{\Omega}_2).$$

and

$$A_1(r) = \exp[b_x(r)],$$

$$A_2(r) = r^2\{\exp[b_\pi(r)] - \exp[b_x(r)]\},$$

$$A_3(r) = A_2(r)/r^2,$$

$$A_4(r) = \exp[b_T(r)] - \exp[b_x(r)] - A_2(r),$$

$$A_5(r) = 2[\exp b_L(r) - \exp b_\pi(r)] - 5.4A_4(r) - 4A_2(r),$$

$$A_6(r) = 3.158 \times 10^5 C(r) r^{-5},$$

$$A_7(r) = 3.158 \times 10^5 C(r) r^{-6},$$

$$A_8(r) = -3.663 \times 10^7 C(r) r^{-8},$$

where the distances are measured in a.u., and $b_L(r)$, $b_x(r)$, $b_\pi(r)$ and $b_T(r)$ are defined as follows:

For $r < 5$ a.u.,

$$b_L(r) = 15.4381 - 1.7532r,$$

$$b_\pi(r) = 13.8444 - 1.2827r - 0.0470916r^2,$$

$$b_T(r) = 13.6828 - 1.10567r - 0.078402r^2,$$

$$b_x(r) = 13.5979 - 1.15432r - 0.06737r^2,$$

For $r > 5$ a.u.,

$$b_L(r) = 16.2815 - 1.9219r,$$

$$b_\pi(r) = 17.04057 - 2.29199r + 0.026851r^2,$$

$$b_T(r) = 15.40474 - 1.84207r,$$

$$b_x(r) = 15.4541 - 1.8624r,$$

and

$$C(r) = \{1 + \exp[-4(r - 3.5)]\}^{-1},$$

$$B_1 = 1.0,$$

$$B_2 = (\hat{\Omega}_1\cdot\hat{r})^2 + (\hat{\Omega}_2\cdot\hat{r})^2,$$

$$B_3 = (\hat{\Omega}_1\cdot\hat{\Omega}_2)^2,$$

$$B_4 = B_2 + 0.7(\hat{\Omega}_1\cdot\hat{r})(\hat{\Omega}_2\cdot\hat{r})(\hat{\Omega}_1\cdot\hat{\Omega}_2),$$

$$B_5 = \tfrac{1}{2}(\hat{\Omega}_1\cdot\hat{r})^2(\hat{\Omega}_2\cdot\hat{r})^2,$$

$$B_6 = 0.04805[1 - 5((\hat{\Omega}_1\cdot\hat{r})^2 + (\hat{\Omega}_2\cdot\hat{r})^2 + 3(\hat{\Omega}_1\cdot\hat{r})^2(\hat{\Omega}_2\cdot\hat{r})^2) + 2(\hat{\Omega}_1\cdot\hat{\Omega}_2 - 5(\hat{\Omega}_1\cdot\hat{r})(\hat{\Omega}_2\cdot\hat{r}))^2]$$

$$B_7 = -0.2002[(\hat{\Omega}_1\cdot\hat{\Omega}_2) - 3(\hat{\Omega}_1\cdot\hat{r})(\hat{\Omega}_2\cdot\hat{r})]^2 - 1.672[(\hat{\Omega}_1\cdot\hat{r})^2 + (\hat{\Omega}_2\cdot\hat{r})^2] - 11.133,$$

$$B_8 = 1.0.$$

The energy unit is °K.

References

1. A. J. Berlinsky and A. B. Harris, *Phys. Rev. Lett.*, **40,** 1579 (1978).
2. S. F. O'Shea and M. L. Klein, *Chem. Phys. Lett.*, **66,** 381 (1979).
3. P. R. Kubik and W. N. Hardy, *Phys. Rev. Lett.*, **41,** 257 (1978).
4. S. C. Wang, L. Senbetu and C.-W. Woo, *Phys. Rev. B.*, **20,** 3641 (1979).

5. S. C. Wang, L. Senbetu and C.-W. Woo, to be published in *J. Low Temp. Phys.*
6. D. N. Lowy and C.-W. Woo, *Phys. Rev. B.*, **13**, 3790 (1976), and T. Li, X. Sun and C.-W. Woo, to be published in *Phys. Rev.*
7. W. E. Carlos and M. W. Cole, *Surf. Sci.*, **77**, 173 (1978).
8. G. Boato and G. P. Felcher, private communication. L. Mattera, F. Rosatelli, C. Salvo, F. Tommasini, U. Valvusa and G. Vidali, *Surf. Sci.*, **93**, 515 (1980).
9. L. Zandee, J. Verberne and J. Reuss, *Chem. Phys.*, **26**, 1 (1977).
10. R. D. Etters, R. Danilowicz and W. England, *Phys. Rev. A.*, **12**, 2199 (1975).